

The Language of Lava: Updated models for folded Venusian flows, lava rheologies, and surface roughnesses.

S.E.H. Sakimoto¹ and, T.K.P. Gregg², ¹Space Science Institute, Boulder, CO 80301 (ssakimoto@spacescience.org)

²Dept. of Geology, University at Buffalo, Buffalo NY 14260 (tgregg@buffalo.edu).

Introduction: Folding on basaltic lava flow surfaces is common on Earth, although not ubiquitous: to form folds, there must be a balance between the rate of crust thickening (a function of cooling rates, which is related to ambient conditions) and lava flow velocity (a function of effusion rate and underlying slopes) [1-3] (Fig. 1). The fold amplitude and wavelengths have the potential to reveal important information about the flow velocities during emplacement.

Folded lava flows are uncommon on Venus, although the best spatial resolution of Magellan synthetic aperture radar (SAR) is 75 m/px [4]. Thus, fold wavelengths less than ~100 m will not be observed, although their properties may be recorded in radar roughness or backscatter. On Earth, folds with these wavelengths are more common on evolved composition lavas [5], but this may not be the case on Venus [6]. Venusian large-scale folds (Fig. 2) may have significantly different radar roughness than smooth, pahoehoe-type flows with potential small-scale folds (Fig. 3).

As lava flows advance, their surface crust deforms. For a subset of flows, pronounced sets of parallel folds perpendicular to the flow direction form at a dominant wavelength, and continued flow and deformation may allow longer wavelength second generation folds [3].

Fold wavelength is thought to depend primarily of the ratio of the surface crust viscosity to that of the still-molten lava interior, along with crust thickness [1,3,5]. Both viscosity and crust thickness are dependent on lava composition; the crustal growth rate during emplacement is also controlled by the cooling environment [2].

Folded flows could potentially generate distinctive radar backscatter signatures under appropriate illumination directions and if fold wavelengths are near radar wavelengths [7,8]. Folds are common on basaltic terrestrial pahoehoe flows, and basaltic terrestrial folds occupy a distinctive wavelength range. For terrestrial lava radar returns, surface roughness has a strong controlling

influence on radar brightness [9], although distinguishing between pahoehoe flow types is difficult in, for example, Shuttle Imaging Radar [10], but has had some success in Airborne Synthetic Aperture Radar (AIRSAR) L-Band (24-cm wavelength, 10 m/pixel resolution) datasets [11]

However, reported wavelengths for more evolved compositions cluster in the same wavelength range. Some authors dispute the ability of evolved compositions to produce ductile shortening and folds [12] and thus suggest that the fold analysis approach should

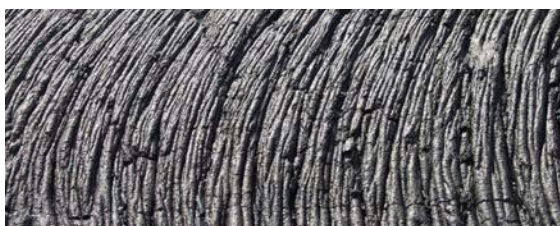


Figure 1. Example of a terrestrial (Eastern Snake River Plains) folded flow surface (pahoehoe lava). Image is 1.5 m across (Photo by Sakimoto).

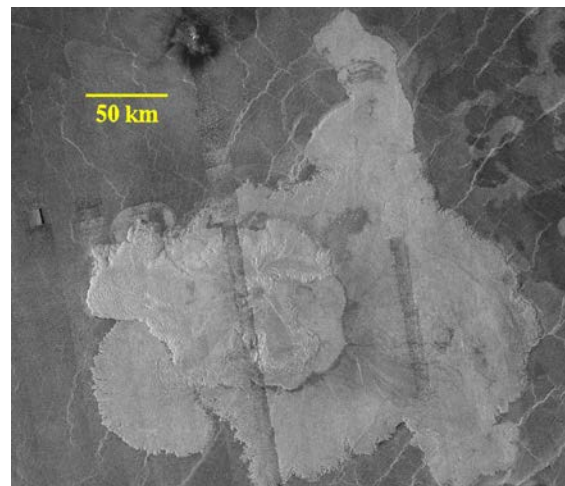


Figure 2. Mahuea Tholus (37.3°S, 165.1°E), Venus, displaying radar-bright ridged flows that have been interpreted to be folds [18]. Image courtesy of NASA/JPL/LPI.

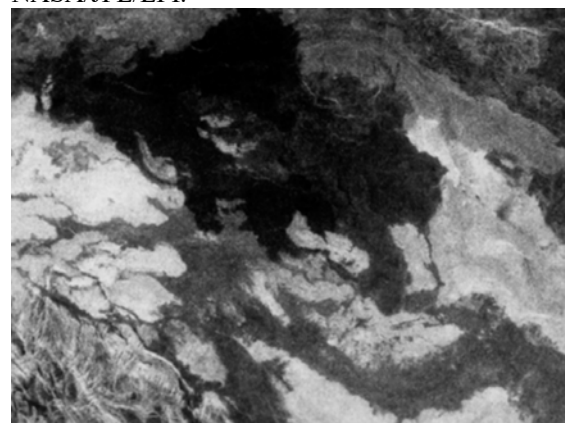


Figure 3. Venusian radar dark lava flow (top center) in Lavinia Planitia (55°S, 354°E) inferred to have a smooth surface similar to terrestrial pahoehoe flows. Magellan F-MIDR 175 km across. Image courtesy of NASA PDS Imaging node.

potentially be limited to basaltic compositions. Recent investigations into Ovda Fluctus (6.1°S, 95.5°E), a Venusian flow complex that displays “festoons” or arcuate folds, concluded that the fluctus is likely not composed of evolved lavas—despite the large festoons [6].

Background: Prior studies used dimensionless analysis to define two dimensionless parameters governing the presence of folding in a material with viscosity decreasing exponentially with depth [1]: R is a ratio of surface (η_o) and interior (η_i) viscosities, and S is a ratio of gravitational forces damping folding to compressive forces enhancing folding, given by:

$$S = \rho g(1/\gamma) / [4\eta_o(-\epsilon_{xx})]$$

where ρ is flow density, g is acceleration of gravity, γ is an inverse length scale related to dominant fold wavelength, η_o is surface viscosity, and $-\epsilon_{xx}$ is the strain rate parallel to flow direction [1,3]. Gregg et al. [3] showed that these relationships are applicable to laboratory PEG simulations as well as basaltic terrestrial flows, and that—when applied to martian and Venusian flows—more evolved compositions may be implied [13]. However, given cautions raised for folds on lavas with evolved compositions [12], and the simplifying assumptions included in these analyses, it is worthwhile to use new advances in modeling free surfaces to investigate the predicted behavior of basaltic flow surfaces.

Methods: We use COMSOL 6.0 multiphysics [14] to solve the incompressible 2-D momentum and continuity equations directly for the velocity field, and the 2D energy equation for the temperatures. We compute surface strain rates from the solutions to enable dimensionless parameter comparisons with the existing studies. A temperature-dependent rheology is necessary to calculate the viscosity distribution resulting from convective and radiative cooling: the velocity and temperature solutions are coupled through the rheology. All solutions are two-phase flow, with a lower lava domain and an upper atmosphere domain, a lava-air interface. We model for both terrestrial and Venusian ambient surface conditions. Additionally, for comparison with existing work, we model an isothermal basaltic fluid with an imposed exponential viscosity decrease within the flow, and examine deformation wavelengths as a function of surface strain rate. We test several computational approaches to modeling the time dependent surface deformation. All three are strongly dependent on surface tension, but surface tensions of basaltic melts are not strongly dependent on either melt composition or the atmosphere within the apparatus [2, 15], with experimental values within the 0.35–0.37 N m⁻¹ range.

Results: The *moving mesh* approach is generally suggested as the first approach to deforming surfaces, but although it is quicker, it does not explicitly account

for the atmosphere above the lava surface (a minor problem), nor does it deal well with surface topology changes past minor folding (a larger problem).

The *level set*, *phase field interface* approaches are more computationally expensive but better suited to dealing with larger surface topology changes. The initial results indicate that the relatively large lava surface tension values relative to the gravitational and deformation forces are better modeled in the *phase field interface* than the *level set* method, and that as fold amplitude grows past initial perturbation-type amplitudes, it is necessary to use adaptive mesh refinement to generate a denser mesh at the flow surface.

We find that two processes produce a significant change in predicted lava fold wavelengths. First, differences in cooling rates can produce a viscosity profile that is significantly different than the exponential viscosity decrease assumed in prior work. Second, lava rheology (either temperature dependence or strain rate dependence) can affect both the viscosity profile and the surface strain rate. Different rheology models [e.g. 16,17] generate somewhat different folding results.

Summary: Folding of lava flow surfaces is a complicated process but has the potential to reveal important information about emplacement parameters, including rheology and strain rate. Previous models used to interpret surface folds have relied on simplifying assumptions that are maddeningly interrelated, making unique interpretations impossible. By using COMSOL to folded lava flows, we will be able to provide interpretation of folded flows more discretely linked to flow properties and flow emplacement physical processes.

References: [1] Fink, J.H. and R.C. Fletcher (1978) *JVGR* 4(1-2):151-170. [2] Fink, J.H. and Griffiths, R.W. (1990) *J. Fluid Dynamics* 221:485-509. [3] Gregg, T.K.P. et al. (1998) *JVGR* 80:281-292. [4] Saunders, R.S. et al., (1992) *JGR*, 97(E8):13067-13090. [5] Fink, J.H. (1980) *Geology* 8:250-254. [6] Wroblewski, F.B. et al. (2019) *JGR* 124(8):2233-2245. [7] Martel, L., and R. Greeley (1985) *LPSCXVI*, p. 521. [8] Gaddis, L.R., et al. (1990) *Photogramm. Eng. Remote Sensing*, 56(2), pp.211-224. [9] Campbell, B.A. and M.K. Shepard (1996) *JGR* 101(E8) 18941-18951. [10] Gaddis, L., et al., (1989) *GSA Bull.* 101:317-332. [11] Tolometti, G.D., et al., (2020) *Planet. Space Sci.* 190:104991. [12] Andrews, D.M. et al. (2021) *EPSL* 553:116643. [13] Warner, N.H. and Gregg, T.K., (2003) *JGR* 108(E10). [14] COMSOL Multiphysics v. 6.0 (2021) www.comsol.com. [15] Walker, D. and O. Mullens Jr. (1981) *Contr. Min. Petrology* 76:455-462. [16] Sehlke, A. and A.G. Whittington (2016) *Geochim. Cosmo. Acta*, 191, pp.277-299. [17] Morrison, A.A., et al. (2019). *Icarus*, 317, pp.307-323. [18] Moore, H.J. et al. (1992) *JGR* 97(E8);13,479-13,493.